

Residual stresses in planar solid oxide fuel cells

W. Fischer*, J. Malzbender, G. Blass, R.W. Steinbrech

Research Center Jülich GmbH, Institute for Materials and Processes in Energy Systems, 52425 Jülich, Germany

Received 29 September 2004; received in revised form 4 February 2005; accepted 7 February 2005

Available online 31 May 2005

Abstract

The in-plane residual stress distribution in the electrolyte of an anode-supported planar solid oxide fuel cell has been determined using X-ray powder diffraction. Measurements have been carried out with half cells in green state, after co-firing and after anode reduction. The residual stress in the electrolyte is compressive. Values of about -560 MPa are determined at room temperature for an approximately $10\ \mu\text{m}$ thick electrolyte layer on an oxidized ~ 1.5 mm thick anode substrate, independent of location. Chemical reduction of the anode leads to a slight decrease of the compressive electrolyte stress to -520 MPa. At operation temperature ($800\ ^\circ\text{C}$) the stress is by a factor of about two lower, but remains compressive. The electrolyte results are used to calculate the residual stress in the oxidized and in the reduced anode. Independent of the oxidation state a tensile stress of about 4 MPa is calculated. Implications for anode failure are discussed by comparing this value with the fracture stress of large $200\ \text{mm} \times 200\ \text{mm}$ cells at a failure probability of 10^{-6} .

© 2005 Elsevier B.V. All rights reserved.

Keywords: Solid oxide fuel cell; Ytria-stabilized zirconia; Residual stress; X-ray diffraction; Thermoelastic modeling

1. Introduction

Solid oxide fuel cells (SOFCs) are electrochemical devices for high efficiency energy conversion. Several concepts of practical realization are currently under development [1]. At the Research Center Jülich (FZJ) the anode-supported planar SOFC concept with thin electrolyte has matured to a level that operation of stacks with an electrical power output of ~ 13 kW could be demonstrated [2]. A single cell used in such stacks is a layered composite (Fig. 1). At FZJ an approximately 1.5 mm thick porous $\text{ZrO}_2(8\ \text{mol}\% \text{Y}_2\text{O}_3)/\text{NiO}$ anode substrate supports four functional layers, anode functional layer (AFL), electrolyte, cathode functional layer (CFL) and cathode current collector (CCC). The AFL has the same composition as the substrate but higher density. The ion-conducting dense electrolyte contains $8\ \text{mol}\%$ yttria-stabilized zirconia (8YSZ) and has a thickness of about $10\ \mu\text{m}$. Lanthanum Strontium Manganite (LSM) is used as standard materials for the two cathode layers.

Besides the electrochemical criteria, e.g. power density and degradation, the mechanical integrity of the electrolyte under service conditions and during thermal cycling is crucial for the successful operation of the cell. To ensure a failure free electrolyte layer during manufacturing and operation critical tensile stresses which exceed the fracture stress have to be avoided. In this respect, thermal mismatch stress which keeps the electrolyte layer under compression appears to be advantageous. They are conveniently obtained by co-firing of anode and electrolyte [3]. However, there is still little information on the quantitative level of residual stresses obtained with anode supported, thin electrolyte SOFCs. Also studies of the local in-plane stress distribution are missing.

In this study X-ray powder diffraction is used to map the stress distribution in the electrolyte layer of a half cell, i.e. anode substrate and electrolyte with intermediate thin AFL [4,5]. The residual stress after four processing steps is measured, (i) green state, (ii) co-firing, (iii) co-firing and flattening and (iv) reduction of anode. The determined electrolyte stress is then used to calculate with thermoelastic curvature data [6] the stress at $800\ ^\circ\text{C}$ in the oxidized and in the reduced

* Corresponding author. Tel.: +49 2461 615052; fax: +49 2461 618178.
E-mail address: w.fischer@fz-juelich.de (W. Fischer).

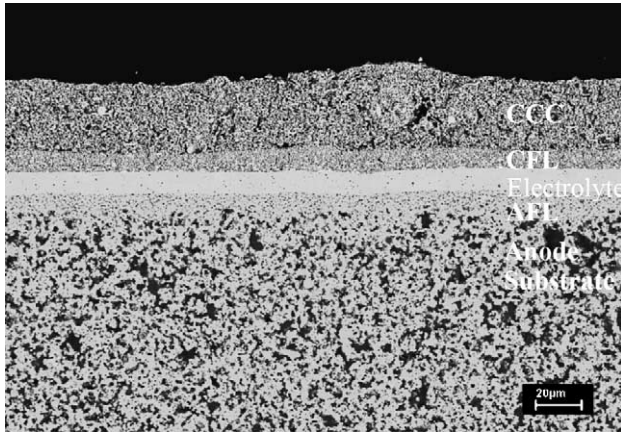


Fig. 1. Cross-section of a SOFC cell.

anode. Finally, the residual anode stress is compared with the fracture stress of the anode material. The conservative estimate also considers large cells and low failure probability of the SOFC.

2. Experimental

The materials, deposition and compaction technologies used for manufacturing of SOFCs at FZJ are schematically depicted in Fig. 2. The current study focuses only on the manufacturing steps related with the electrolyte layer (center of Fig. 2). Anode functional layer and electrolyte are deposited on a pre-sintered (1250 °C) porous anode substrate by vacuum slurry coating. The composite is then co-fired at

1400 °C to obtain a dense electrolyte (Fig. 3). Depending on the sintering shrinkage of electrolyte and anode substrate, the co-firing can result in half cells with curved shape. An additional high temperature flattening by mechanical load has proved to successfully remove the slight warp. However, cooling down of the co-fired, flattened half cells to SOFC operation and room temperature typically generates thermoelastic cell curvature. The curvature reflects the thermoelastic mismatch between the layers of the half cell and is indicative of existing residual stresses. Also the reduction step of the anode changes the curvature of the half cell and influences the residual stress due to volume change and softening. To avoid cracking of the dense electrolyte, it is mechanically advantageous if the electrolyte remains at least up to operation temperature under compressive stress. But on the other hand the compressive stress should not exceed the strength of YSZ under compression, which is about 1 GPa [7]. In order to get more insight into the electrolyte stress state, we investigated the stress distribution after subsequent manufacturing steps:

1. as-deposited (stress-free, check of the experimental set-up),
2. after co-firing at 1400 °C/5 h/air,
3. after an additional ‘flattening’ procedure (1360 °C/1 h/air/mechanical load 10 N),
4. after reduction of NiO to Ni in the substrate at 900 °C/10 h in 4 vol.% H₂/Ar.

The X-ray measurements were carried out with a single half-cell specimen at room temperature. The standard $\sin^2 \psi$ method in ψ -geometry was employed for measurement of the lattice strain in the polycrystalline 8YSZ electrolyte. To get enough intensity for a local resolution of about 1 mm²

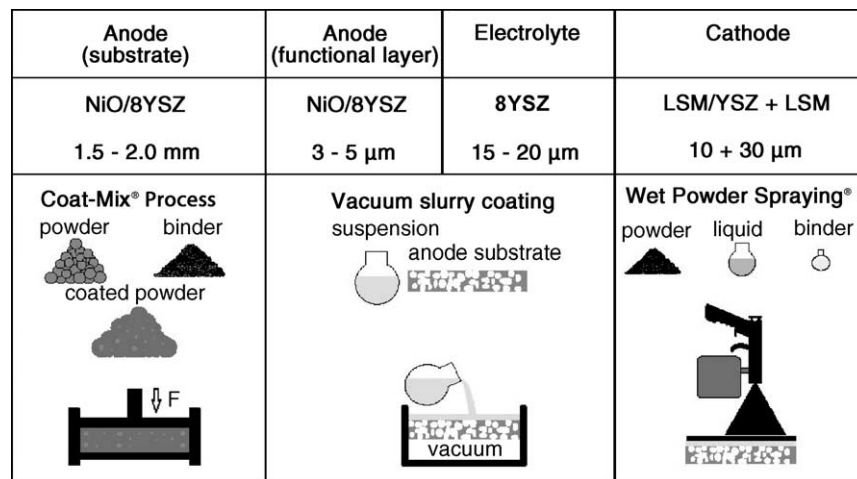


Fig. 2. Materials and technologies used for manufacturing planar SOFCs.

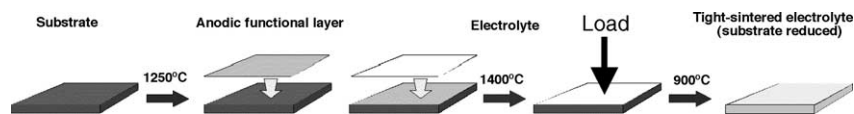


Fig. 3. Processing steps influencing the residual stress state in a SOFC half cell.

a polycapillary semi-lens was mounted in the incident beam path. The parallel beam behind the semi-lens was collimated to $0.6 \text{ mm} \times 1 \text{ mm}$ by crossed slits. The final dimensions of the cell after co-firing were $55 \text{ mm} \times 55 \text{ mm} \times 2 \text{ mm}$. The lattice strain in the electrolyte layer was measured in a central $50 \text{ mm} \times 50 \text{ mm}$ area divided into a grid of 10×10 equidistant points. X-ray elastic constants of Eigenmann et al. [8] were used for converting strain to stress. The stress was determined assuming a plane unidirectional stress field. Further experimental details and the methods applied for the data evaluation are compiled in Table 1.

3. Results and discussion

The stress distribution after the different manufacturing steps is displayed graphically in Fig. 4. For visualization, stress values are coded in such a way that the stress spread over the whole gray scale key equals to 200 MPa in all graphs. This ensures the comparability of fluctuations after the different manufacturing steps. Dark color corresponds to a low

Table 1

Experimental details and X-ray diffraction data evaluation

Diffractometer	Philips X'Pert MRD 3050/65 with Eulerian cradle and motorized sample stage
Radiation	Cu K, 40 kV/50 mA
Primary optics	K β filter, polycapillary half-lens, cross slit collimator $0.6 \text{ mm} \times 1 \text{ mm}$
Reflection, 2θ range	Reflection (6 2 0), $140\text{--}146.5^\circ$, $\Delta 2\theta = 0.05^\circ$, 10 s/step
Method	ψ tilt, $\sin^2 \psi \leq 0.5$, equidistant in $\sin^2 \psi$
Corrections	Absorption, linear background, Lorentz polarization, Rachinger $K\alpha_2$ subtraction
Peak position	Center of gravity, parabola fit, manual
Elastic constants	$E_{(620)} = 215 \text{ GPa}$, $\nu_{(620)} = 0.29$
X-ray elastic constants	$s_1 = -1.35 \text{ TPa}^{-1}$, $1/2s_2 = 6.0 \text{ TPa}^{-1}$

stress value; bright color indicates a high stress value. Additionally, the mean stress and the standard deviation are given for each map.

The representation of the stress in Fig. 4a (electrolyte as-deposited) may also be taken as a check of the experimental set-up, including data evaluation. The electrolyte layer, as deposited by vacuum slurry coating before sintering can

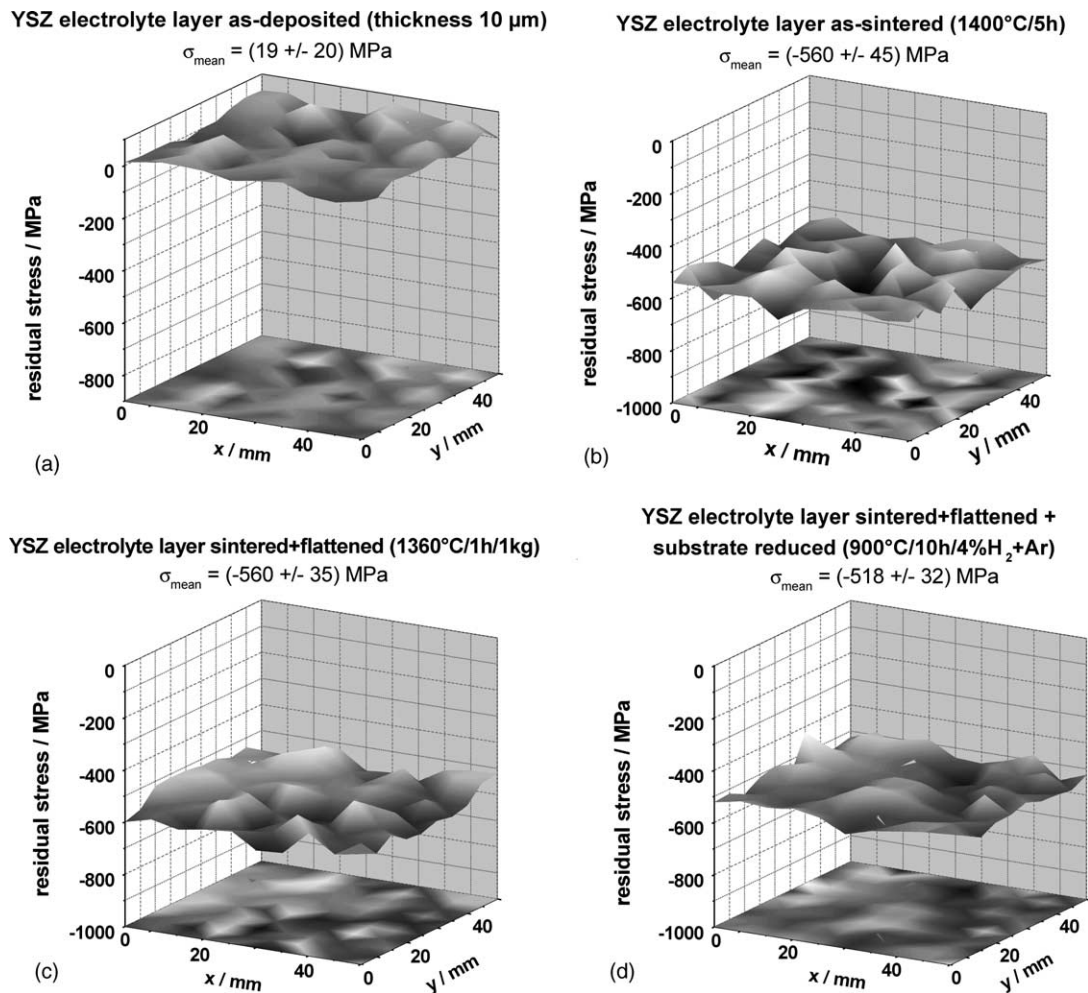


Fig. 4. Residual stress distributions in the electrolyte layer after subsequent steps of the manufacturing of a half cell: (a) electrolyte as-deposited, (b) co-fired, (c) co-fired and flattened, and (d) co-fired, flattened and finally reduced. Same half cell specimen used for all experiments.

assumed to be in a stress free state, since it is only a sediment of 8YSZ powder particles. Hence, the plot also serves as indicator for the precision of the strain measurement.

The results for the electrolyte after atmospheric sintering at 1400 °C for 5 h are shown in Fig. 4b. The electrolyte exhibits a strong compressive stress of about -560 MPa at room temperature. This stress is independent of the in-plane cell location. The fluctuation including experimental uncertainty is 45 MPa.

During sintering frequently a slight warpage of the cell composite plates occurs, which remains with cooling and is superimposed to the thermoelastic curvature. Commonly a high temperature flattening procedure is added to the co-firing, but this procedure might imply crack formation. Respective defects should be reflected in a change of the electrolyte stress. Fig. 4c shows the stress distribution in the electrolyte layer after the flattening step. The overall stress level at room temperature remains unchanged at about -560 MPa. Hence, stress distribution does not differ from that before flattening. The result confirms, that at 1360 °C the anode/electrolyte composite can be plastically deformed to eliminate warp. The in-plane stress fluctuation of the flattened half cell is slightly reduced (35 MPa), which might be an indication of defect healing.

After deposition of the cathode layers on the SOFC half cells they are typically sintered under oxidizing atmosphere. Thus anode reduction is required before stack operation to obtain the necessary electron conductivity. In the present case a chemical reduction of NiO to Ni at 900 °C for 10 h in a 4% H₂/Ar was chosen. Thereby the volume and the physical properties of the anode material are affected. Consequently, the residual stress in the electrolyte also changes. Numerous SEM investigations of the electrolyte surface as well as of cross-sections of half cells to check the influence of these manufacturing steps on the microstructure did not indicate a micro-crack formation. Fig. 4d shows the stress distribution after anode reduction. The level of the compressive stress has slightly decreased to -520 MPa. The stress is essentially constant across the entire cell. The in-plane stress fluctuation is further reduced to about 30 MPa.

Comparison of the obtained results with literature turns out to be difficult, since only little information is available. However, synchrotron radiation has been used recently to determine with a local approach residual stresses in the electrolyte of anode-supported SOFCs [9]. Cells with slightly different anode geometry (2 mm) and electrolyte thickness (about 20–40 μm) were analyzed. An effect of the in-plane position on the stress was reported which could not be verified by our observations. Nevertheless, the compressive stress was -660 ± 20 MPa for oxidized, flattened cells and -670 ± 10 MPa for reduced cells [9], i.e. in the same order of magnitude like the present results.

From the results of both diffraction studies the measured compressive residual stress in the electrolyte appears high enough to provide a mechanically robust electrolyte layer. However, it is also important that the compressive stress at

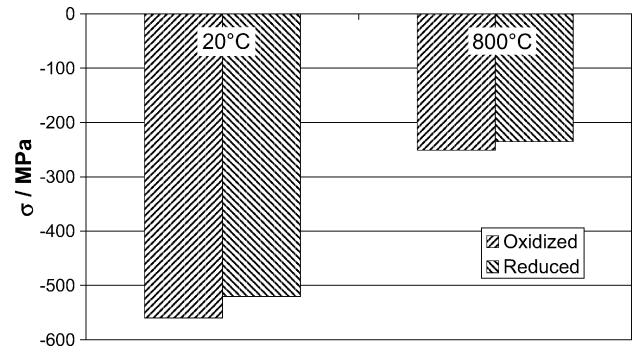


Fig. 5. Residual stress in the electrolyte layer at room and operation temperature. Slight shift between electrolyte stress for oxidized and reduced anode. High temperature (800 °C) data derived from X-ray measurement at room temperature and temperature dependent thermoelastic parameters from curvature experiments [6].

operation temperature (~ 800 °C) is sufficient, too. Fig. 5 compares the RT results with 800 °C stresses, theoretically derived from the RT X-ray data by considering the temperature dependence of thermoelastic properties determined in curvature experiments [6]. The stresses in the oxidized and in the reduced anode state decrease similarly. At operation temperature (800 °C) the electrolyte is still under compression by a fairly high residual stress of about -240 MPa. With such a compressive residual stress a malfunction of a cell due to crack formation should not occur.

The electrolyte stresses determined above can also be used to estimate the stresses in the anode [10]. The results indicate a stress gradient in the oxidized anode. A compressive stress of -7.5 MPa exists at the free surface and a tensile stress of 15 MPa at the interface with the electrolyte. The dependence of the anode stress on the relative position with respect to the electrolyte is a result of the curvature of the cells. In the case of a cell constrained against deflection, like fixed cells in a stack, the average anode tensile stress becomes 4 MPa. Similar gradients with slightly lower values are determined in the reduced anode, the average stress in the constraint case is again ~ 4 MPa. At SOFC operation temperature the stress decreases to ~ 2 MPa, essentially independent of oxidized or reduced anode state.

The change in stress during reduction is a result of the shrinkage in volume as the NiO is reduced to Ni and the change in stiffness. A reduced anode has a lower stiffness than an anode in the oxidized state. Hence the shrinkage leads to an increase whereas the decrease in stiffness to a decrease in stress. The results presented here suggest that both effects compensate and the finally reduced cell shows a similar stress magnitude in the electrolyte as the oxidized cell. Hence no stress increase during reduction is obtained and micro-cracking is unlikely.

Considering the favorable compressive stress in the electrolyte layer of co-fired SOFC the discussion of the mechanical integrity can be restricted to the anode properties. Indeed, for co-fired cells the critical layer in tensile stress state is the anode [6]. Compared to anode fracture stresses in the order

of 50–100 MPa the average tensile residual stresses appear to be rather low and not critical. However, if in addition applied tensile stresses due to cell fixation in the stacks are taken into account the difference to the fracture stress might diminish. Moreover, the statistics of flaw distribution (Weibull modulus), stressed anode volume and type of loading are important [11]. For example, an increase in cell size with the statistical probability of larger defects being then present can result in a significant drop of fracture stress compared to small specimens under the same thermoelastic residual stress. Such statistical aspects of the flaw size distribution have been addressed previously [11]. Moreover, the anodes experience a tensile loading rather than bending, under which specimens are conveniently tested. Both effects lead to a reduction of the critical stress for a discrete fracture probability [11]. Hence, an assessment of the failure relevance of the residual tensile anode stresses determined above requires statistically reliable mechanical testing of the cells. For example, using four-point bending a room temperature fracture stress of ~ 84 MPa and a Weibull modulus of ~ 13 was obtained for reduced specimens of an area of 100 mm^2 [12]. Considering anodes of $200 \text{ mm} \times 200 \text{ mm}$ under tensile loading, a fracture stress of ~ 14 MPa for a failure probability of 10^{-6} is obtained [11]. The above estimates reveal that in the present case the critical fracture stress is still significantly larger than the residual stress in the reduced anodes at room temperature.

4. Conclusions

Two-dimensional residual stress patterns of the YSZ electrolyte in SOFCs were measured using X-ray powder diffraction. With the method a lateral resolution of about 1 mm was achieved using standard X-ray diffraction equipment, and applying a polycapillary semi-lens in the incident beam path. The stress state of the $10 \text{ }\mu\text{m}$ thick electrolyte in planar SOFCs of FZJ is mainly governed by the supporting anode substrate. Values of about -560 MPa are determined for the electrolyte layer on an oxidized anode substrate independent of location. The flattening procedure applied to the SOFCs to remove the slight warp, existing from co-firing, does not

essentially change the residual stress level but decreases the in-plane fluctuation. Chemical reduction of NiO to Ni in the porous anode substrate lowers the absolute stress level in the electrolyte by 10%. A calculation of the anode stress resulted in values of ~ 4 MPa. A combination of the measured electrolyte stress with calculations using the temperature dependent thermal expansion coefficients of electrolyte and anode shows that the electrolyte layer remains under a favorable high compressive stress of ~ -240 MPa, at operation temperature ($800 \text{ }^\circ\text{C}$). Again, the anode experiences on average only a low tensile stress (~ 2 MPa).

References

- [1] S.C. Singhal, *Solid-State Ionics* 152 (2002) 405–410.
- [2] R. Steinberger-Wilckens, I.C. Vinke, L. Blum, J. Rimmel, F. Tietz, W.J. Quadackers, in: M., Mogensen (Ed.), *Proceedings of the Sixth European SOFC Forum*, Lucerne, Switzerland, 2004, p. 11.
- [3] P. Batfalsky, H.P. Buchkremer, D. Froning, F. Meschke, H. Nabelek, R.W. Steinbrech, F. Tietz, *Proceedings of the Third IFCC*, Nagoya, Japan, 1999.
- [4] V. Hauk, *Structural and Residual Stress Analysis by Nondestructive Methods, Evaluation – Application – Assessment*, Elsevier, 1997.
- [5] V. Hauk, H. Hougardy, E. Macherauch, *Proceedings of the Conference on Residual Stresses*, Darmstadt, 1990. Deutsche Gesellschaft für Materialkunde – DGM Informationsgesellschaft mbH, Oberursel, 1991, pp. 3–20.
- [6] J. Malzbender, T. Wakui, R.W. Steinbrech, L. Singheiser, in: M., Mogensen (Ed.), *Proceedings of the Sixth European SOFC Forum*, Lucerne, Switzerland, 2004, p. 329.
- [7] T. Kato, N.S. Wang, A. Negishi, A. Momma, Y. Kasuga, A. Nozaki, *Proceedings of the Third International Fuel Cell Conference*, Nagoya, Japan, 1999, p. 461.
- [8] B. Eigenmann, B. Scholtes, E. Macherauch, *Materialwiss. Werkstofftech.* 20 (1989) 314–325.
- [9] H. Yakabe, Y. Baba, T. Sakurai, Y. Yoshitaka, *J. Power Sources* 135 (2003) 9–16.
- [10] J. Malzbender, *Appl. Phys. Lett.* 84 (2004) 4661–4662.
- [11] J. Malzbender, R.W. Steinbrech, L. Singheiser, in: S.C., Singhal, M., Dokiya (Eds.), *Proceedings of the SOFC VIII, 203rd Meeting of the Electrochemical Society*, Paris, 2003, p. 1463.
- [12] J. Malzbender, L. Singheiser, R.W. Steinbrech, *29th International Conference on Advanced Ceramics and Composites*, January 23–28, 2005, Cocoa Beach, FL, USA, in press.